Joint Linear Precoding and Beamforming for the Forward Link of Multi-Beam Broadband Satellite Systems

Bertrand Devillers* , Ana Pérez-Neira† and Carlos Mosquera‡
*Centre Tecnològic de Telecomunicacions de Catalunya (CTTC), Castelldefels, Barcelona, Spain.
†Dept. of Signal Processing and Communications, Universitat Politècnica de Catalunya, Barcelona, Spain.
‡Signal Theory and Communications Department, University of Vigo, Vigo, Spain.
Emails: bertrand.devillers@cttc.es, ana.isabel.perez@upc.edu, mosquera@gts.uvigo.es

***Abstract*—Next generation high throughput satellite systems are expected to rely on the deployment of a high number of beams in the user link, and therefore operate in an interference limited regime. This paper builds on the combination of advanced interference mitigation techniques and ground based beamforming to cope with this increased level of interference among users. Focussing on the forward link of a multi-beam broadband satellite system, we consider the joint design of linear precoding and ground based beamforming at the gateway. This joint design is modeled, and different linear precoding techniques are considered for comparison. The provided simulation results quantify the performance gain generated by this joint design with respect to considering precoding for a fixed on-board beamforming. The robustness of the considered scheme to channel estimation errors is also analyzed.**

I. Introduction

A key enabler for high throughput next generation satellite communication systems is the deployment of a high number of beams in the link between the satellite and the user terminals (UTs), i.e. the user link. Current generation satellites at Ka-band produce of the order of 80-100 beams to cover Europe, while this value could be up to doubled if unprecedentedly high throughput levels are targeted. The underlying principle is quite simple and well-known in terrestrial cellular systems: the overall system bandwidth can be artificially increased by reusing the same frequency band among various beams of the satellite's coverage area, potentially leading to a proportional increase in system throughput.

However, several issues appear as the number of beams increases. In particular, the system performance becomes limited by the increased level of interference among users situated in distinct beams, due to the side lobes of the beams' radiation patterns. In order to deal with this increased level of interference, current generation satellite systems rely on deploying a well-chosen pattern in the reuse of frequencies among beams: typically, beams with adjacent footprints operate on different frequency bands (or orthogonal polarizations), as they strongly interfere with each other. In this context, an essential parameter is the number of colors N_c in the frequency reuse pattern ($N_c \in \mathbb{N}^+$, $N_c \geq 1$), which we define as the cardinality of the set of disjoint frequency bands used on the cluster of beam footprints which define the coverage area. On the one hand, the lower N_c, the higher the overall system bandwidth will be. On the other hand, the higher N_c, the lower the inference level will be. The current practice typically considers values of $N_c = 3$ or 4, which usually reach the best trade-off and achieve a high system throughput at a desired system availability.

More advanced *interference mitigation techniques* have been considered in a past study of the European Space Agency (ESA) [1], [2]. The objective was to analyze whether full frequency reuse ($N_c = 1$) could be achieved at the expense of introducing extra signal processing on ground at the gateway (GW). Building on the multi-user multiple-input multiple-output (MIMO) theoretical framework, precoding and multi-user detection techniques were considered for the forward link (GW to UTs) and return link (UTs to GW), respectively. The results were encouraging, as the system throughput was significantly improved with respect to a reference scenario designed according to the best practice. Still, this throughput enhancement was obtained at the price of a reduced level of availability, which somehow limits the impact that such strategy could have from a practical point of view.

The generation of beams is carried out by the so-called beamforming, whose role is to linearly combine the radiation patterns of each element of the antenna array in order to generate directive beam radiation patterns. Originally, beamforming was considered for on-board implementation (digital or analog). However, the deployment of a high number of beams may be beyond today's state-of-the-art of on-board processing capabilities. An alternative is to realize the forming of beams digitally on ground at the GW. This concept, commonly referred to as *ground based beamforming* (GBBF), is attractive as it reduces the risk associated with the satellite development (since the on-board operations are simplified), and provides a higher degree of flexibility [3]. GBBF implies the transfer to ground (typically in a frequency multiplexed fashion) of all

This work was performed in the context of the framework of SatNEx III through ESA Contract RFQ/3-12859/09/NL/CLP. The work of B. Devillers was also partially supported by the Spanish Government under project TEC2010-17816 (JUNTOS). The work of A. Pérez-Neira has been supported by the Spanish Government under project TEC2008-06327-C03-01 and the Catalan Government under the grant 22009SGR0891

radiating elements signals (feed signals) instead of the beam signals (as it would be the case for on-board beamforming).

The novelty of the present work lies in the combination (in a joint design) of the two above-mentioned concepts: GBBF and interference mitigation techniques. This paper focuses on the forward link of a multi-beam broadband satellite system, and considers the *joint design of linear precoding and beamforming* on-ground, i.e. at the GW. The objective is to quantify the performance gain generated by this joint design with respect to considering adaptive precoding for a fixed beamforming (as in [1], [2]). The paper is organized as follows. Section II presents the signal model, first for the fixed beamforming scenario, and then for the joint precoding and beamforming design. The different precoding solutions considered in this work are described in Section III. Finally, simulation results are presented and analyzed in Section IV, while conclusions are provided in Section V.

Notation: Boldface uppercase letters denote matrices and boldface lowercase letters refer to column vectors. We denote by $(.)^H$ the Hermitian transpose.The $N \times N$ identity matrix is denoted by $\mathbf{I}_N$, and diag $(\mathbf{a})$ builds a diagonal matrix from the elements of the vector $\mathbf{a}$. Nonboldface lowercase letters are used to refer to the entries of a matrix: the (k,l)th entry of the matrix $\mathbf{W}$ is denoted by w_{kl}. Finally, if $\mathbf{D}$ is a diagonal matrix, $\mathbf{D}^{1/2}$ refers to taking the square root of the diagonal elements.

II. System Model

Consider the forward link of a broadband satellite system, where a single GW provides broadband services to a large set of fixed UTs. A transparent satellite payload is assumed. We assume TDMA in the user link such that, in the frequency band of interest, at each time instant the GW is simultaneously serving a total of K users (which constitute a selected subset of users). To this end, the satellite is equipped with an array fed reflector antenna, whose number of elements/feeds is denoted by N. In such scenario, assuming full frequency reuse ($N_c = 1$), the received signal can be modeled as

$$\mathbf{y} = \mathbf{H}_f \ \mathbf{x}_f + \mathbf{n} \tag{1}$$

where $\mathbf{y}$ (resp. $\mathbf{n}$) is a $K \times 1$ vector containing the stack of the received signals (resp. noise components) at each UT. The $N \times 1$ vector $\mathbf{x}_f$ is the stack of the on-board transmitted signals at all feeds. Throughout the paper, the subscript $_f$ will be used to refer to quantities in the feed space, while $_b$ will denote beam space quantities. The user link channel matrix $\mathbf{H}_f$ is of size $K \times N$ and can be decomposed as follows:

$$\mathbf{H}_f = \mathbf{W}\mathbf{G} \tag{2}$$

where:

- $\mathbf{W}$ is a $K \times K$ diagonal matrix modeling the atmospheric fading in the user link.
- $\mathbf{G}$ is a $K \times N$ matrix which accounts for the feed radiation patterns, the path loss, the receive antenna gain and the noise power. Its $(k,n)^{\text{th}}$ entry is modeled as

$$g_{kn} = \frac{G_R \ a_{kn}}{4\pi \frac{d_k}{\lambda} \sqrt{k_B T_R B_W}} \tag{3}$$

with d_k the distance between the k^{th} UT and the satellite, λ the carrier wavelength, k_B the Boltzmann constant, B_W the carrier bandwidth, G_R^2 the UT receive antenna gain, and T_R the receiver noise temperature. Finally, a_{kn} is a complex number referring to the gain (in amplitude) from feed n in direction of the k^{th} UT, such that the corresponding feed transmit gain (in power) is $G_{T,kn} = |a_{kn}|^2$ or $10\log_{10}(|a_{kn}|^2)$ if expressed in dBi. Note that $\mathbf{G}$ has been normalized by the square root of the UT noise power such that the noise samples in (1) are of unit variance: $E[\mathbf{n}\mathbf{n}^H] = \mathbf{I}_K$.

For a fair comparison of all scenarios that will be considered in the sequel, it is critical to define a common transmit power constraint. For this, we assume the following constraint on the average power transmitted at the feed level:

$$E[\mathbf{x}_f^H \mathbf{x}_f] \leq P \tag{4}$$

where P denote the total transmit power.

A. Scenario 1: Linear Precoding & Fixed Beamforming

In this subsection, we introduce the scenario considered in the above-mentioned work [1], [2], i.e. that of linear precoding for a fixed beamforming. It assumes

(i) A fixed (i.e. channel non-adaptive) on-board beamforming

$$\mathbf{x}_f = \mathbf{B} \ \mathbf{x}_b \tag{5}$$

where $\mathbf{B}$ is the non channel adaptive beamforming matrix of size $N \times K$ (assuming that there are as many beams as users), and $\mathbf{x}_b$ is the stack of the on ground transmitted signal in the beam space. Note that a perfectly calibrated and noiseless feeder link is assumed.

(ii) Adaptive linear precoding in the beam space

$$\mathbf{x}_b = \mathbf{F}_b \ \mathbf{s} \tag{6}$$

where $\mathbf{F}_b$ is the $K \times K$ precoding matrix, and $\mathbf{s}$ is a $K \times 1$ vector. The k^{th} entry of $\mathbf{s}$ is the constellation symbol destined to the k^{th} user. Independent unit energy constellation symbols (QPSK, 8PSK, 16APSK or 32APSK, depending on the modulation and coding mode used) are assumed, i.e. $E[\mathbf{s}\mathbf{s}^H] = \mathbf{I}_K$. To comply with the transmit power constraint (4), the precoding matrix $\mathbf{F}_b$ has to satisfy

$$trace\left(\mathbf{B}\mathbf{F}_b\mathbf{F}_b^H\mathbf{B}^H\right) \leq P \tag{7}$$

Using (5) and (6), the signal model (1) becomes

$$\mathbf{y} = \mathbf{H}_f \ \mathbf{B} \ \mathbf{F}_b \ \mathbf{s} + \mathbf{n} \tag{8}$$

$$= \mathbf{H}_b \ \mathbf{F}_b \ \mathbf{s} + \mathbf{n} \tag{9}$$

where $\mathbf{H}_b \triangleq \mathbf{H}_f\mathbf{B}$ expresses the principle of beamforming: the effect of the matrix $\mathbf{B}$ is essentially to linearly combine the radiation pattern of all N feeds to generate K beam radiation patterns.

B. Scenario 2: Joint Linear Precoding & Beamforming

This subsection introduces the signal model of the scenario of interest of this paper. It assumes

(i) No on-board processing. The feed signals $\mathbf{x}_f$ are available on-ground, assuming again a perfectly calibrated, noiseless and non-bandwidth-limited feeder link.
(ii) Linear precoding in the feed space:

$$\mathbf{x}_f = \mathbf{F}_f \ \mathbf{s} \tag{10}$$

with $\mathbf{F}_f$ the $N \times K$ precoding matrix, in terms of which the transmit power constraint (4) becomes

$$trace\left(\mathbf{F}_f \mathbf{F}_f^H\right) \leq P \tag{11}$$

Using (10), the signal model (1) becomes

$$\mathbf{y} = \mathbf{H}_f \ \mathbf{F}_f \ \mathbf{s} + \mathbf{n} \tag{12}$$

Contrasting (8) and (12), we see that $\mathbf{F}_f$ is to be compared to $\mathbf{B}\mathbf{F}_b$. In other words, the precoding in the feed space $\mathbf{F}_f$ is equivalent to a joint beamforming and precoding design[1]. Moreover, since $\mathbf{F}_f$ is of greater size than $\mathbf{F}_b$, it is obvious that considering the beamforming and precoding jointly cannot perform worse than considering them separately. Quantifying whether the joint design generates a substantial gain in realistic conditions is the objective of this paper. The different linear precoding solutions considered in this work are presented next.

III. LINEAR PRECODER DESIGN

In this section, we describe the different linear precoders which have been considered in this work, and whose performance will be contrasted in Section IV.

A. Zero-Forcing Linear Precoder

The zero-forcing (ZF) criterion targets the complete cancelation of the inter-user interference, by precoding with the pseudoinverse of the channel matrix. For the two scenarios presented in Section II, the corresponding expressions are

$$\mathbf{F}_b = \sqrt{\gamma_b}\ \mathbf{H}_b^H (\mathbf{H}_b \mathbf{H}_b^H)^{-1} \tag{13}$$
$$\mathbf{F}_f = \sqrt{\gamma_f}\ \mathbf{H}_f^H (\mathbf{H}_f \mathbf{H}_f^H)^{-1} \tag{14}$$

for the precoding in the beam space and feed space, respectively. The value of the constants γ_b and γ_f have to be such to comply with (7) and (11), respectively. Note that these particular versions of the ZF linear precoders are such that they equalize the signal to noise ratio (SNR) among users.

[1]From now on, we will refer equivalently to "precoding in the feed space" or "joint precoding and beamforming". Similarly, "precoding in the beam space" is equivalent to "precoding for fixed beamforming".

B. Regularized Channel Inversion

The ZF precoders (13)-(14) were obtained by imposing a zero interference constraint at each receive UT. By relaxing this constraint, it was proved in [4] that a regularized inversion of the channel can significantly improve the system's performance. The corresponding precoding matrices are

$$\mathbf{F}_b = \sqrt{\gamma_b}\ \mathbf{H}_b^H \left(\mathbf{H}_b \mathbf{H}_b^H + \frac{K}{P}\mathbf{I}_K\right)^{-1} \tag{15}$$
$$\mathbf{F}_f = \sqrt{\gamma_f}\ \mathbf{H}_f^H \left(\mathbf{H}_f \mathbf{H}_f^H + \frac{K}{P}\mathbf{I}_K\right)^{-1} \tag{16}$$

for the precoding in the beam space and feed space, respectively. Again, the value of the constants γ_b and γ_f have to be such to comply with (7) and (11), respectively.

C. MMSE Precoders Based on the Uplink-Downlink Duality

The most elegant way of considering the design of linear precoders is to use the uplink-downlink duality[2] framework, originally developed for characterizing the sum capacity of the Gaussian Broadcast[3] channel [5]. In particular, minimum mean square error (MMSE) linear precoders can be derived using this framework. The corresponding precoders expressions are

$$\mathbf{F}_b = \left(\mathbf{H}_b^H \mathbf{P} \mathbf{H}_b + \mathbf{I}_K\right)^{-1} \mathbf{H}_b^H \mathbf{D}_b \mathbf{Q}^{1/2} \tag{17}$$
$$\triangleq \mathbf{G}_b \mathbf{D}_b \mathbf{Q}^{1/2} \tag{18}$$
$$\mathbf{F}_f = \left(\mathbf{H}_f^H \mathbf{P} \mathbf{H}_f + \mathbf{I}_N\right)^{-1} \mathbf{H}_f^H \mathbf{D}_f \mathbf{Q}^{1/2} \tag{19}$$
$$\triangleq \mathbf{G}_f \mathbf{D}_f \mathbf{Q}^{1/2} \tag{20}$$

in the beam and feed space, respectively. The matrix $\mathbf{G}_f$ (resp. $\mathbf{G}_b$) is such that $\mathbf{G}_f^H$ (resp. $\mathbf{G}_b^H$) is the MMSE linear receiver of the dual uplink in the feed (resp. beam) space with power allocation given by $\mathbf{P} = \text{diag}\,(p_1, \ldots, p_K)$, where p_k is the power assigned to the kth UT in the dual uplink, with $\sum_{k=1}^K p_k \leq P$. The diagonal matrix $\mathbf{D}_f$ (resp. $\mathbf{D}_b$) has positive diagonal elements and is such that the columns of $\mathbf{G}_f$ (resp. $\mathbf{B}\mathbf{G}_b$) have unitary norm. The matrix $\mathbf{Q} = \text{diag}\,(q_1, \ldots, q_K)$ refers to the power allocation in the downlink, where q_k is the power allocated to the kth UT.

The uplink-downlink duality framework states that there is a one-to-one relationship between $\mathbf{P}$ and $\mathbf{Q}$ (whose closed-form expression is given in [5]) such that (i) the set of signal to interference plus noise ratio (SINR) in the downlink is the same as in the dual uplink, (ii) the total transmitted power is equal in both cases, i.e. $\sum_{k=1}^K p_k = \sum_{k=1}^K q_k$. As a consequence, the precoders (17) and (19) are completely characterized once the uplink power matrix $\mathbf{P}$ is chosen. Two strategies for the design of $\mathbf{P}$ are considered in this paper.

1) UpConst MMSE Precoder: One possible strategy is to have a constant power for all UTs in the uplink: $p_k = P/K$ for $k = 1, \ldots, K$. According to [1], [2], this solution achieves a good compromise between throughput and availability. As in [1], [2], the acronym "UpConst" will be used to refer to this particular linear MMSE precoder.

[2]Which could be renamed return link - forward link duality in this context.
[3]In the parlance of information theory.

TABLE I
CONSIDERED MODULATION AND CODING MODES AND REQUIRED SINR

ModCod mode	Efficiency Info bit / symbol	Required SINR [dB] (with approx. impl. losses)
QPSK_14	0.5	-2.72
QPSK_13	2/3	-1.52
QPSK_12	1	0.73
QPSK_35	1.2	1.93
QPSK_23	4/3	2.83
QPSK_34	1.5	3.78
QPSK_56	5/3	4.83
8PSK_35	1.8	5.33
8PSK_23	2	6.43
8PSK_34	2.25	7.63
16APSK_23	8/3	9.95
16APSK_34	3	11.20
16APSK_45	3.2	12.05
16APSK_56	10/3	12.60
32APSK_34	3.75	14.58
32APSK_45	4	15.08
32APSK_56	25/6	16.18

TABLE II
USER LINK SIMULATION PARAMETERS

Parameter	Value
Satellite height	35786 km (geostationary)
Satellite longitude, latitude	10° East, 0°
Feed radiation pattern $\{a_{kn}\}$	Provided by ESA
Number of feeds N	155
Fixed beamforming matrix $\mathbf{B}$	Provided by ESA
Number of beams	100
Number of users K	100 (one per beam)
UTs location distribution	Uniformly distributed
Carrier frequency	20GHz (Ka band)
Total bandwidth B_T	500 MHz
Number of carriers M	12
Carrier bandwidth B_W	41.67 MHz
Roll-off factor	0.25
Polarization	1
UT antenna gain G_R^2	41.7dBi
UT clear sky $G_R^2/T_{ClearSky}$	17.68dB/K
UT rain delta temperature	221.83K
Fading	Atmospheric only

2) Equal SINR MMSE precoder: Another possible solution is to choose the power allocation variables $\{p_k\}$ in such a way to equalize all users' SINRs. This strategy implies a higher level of complexity. In fact, a double iterative algorithm is needed to find the $\{p_k\}$, as detailed in [6]. This solution maximizes the minimum SINR among UTs, and therefore targets a full system availability.

IV. SIMULATION RESULTS

In this section, the simulations results are presented. First, the simulation setup and parameters are provided. Then, the numerical results are presented successively for perfect and imperfect channel state information (CSI) at the GW.

A. Simulation Setup and Parameters

We will base our analysis on an antenna radiation pattern (i.e. the $\{a_{kn}\}$) and fixed beamforming (i.e. $\mathbf{B}$) which have been provided by ESA in the framework of a study on next generation broadband satellite systems. It corresponds to an array fed reflector antenna with $N = 155$ elements/feeds, which are linearly combined by the beamforming $\mathbf{B}$ to produce $K = 100$ beams covering the European region. The UTs are assumed to be uniformly distributed over the coverage region. However, we impose that the K users served at a given time instant be reasonably spread over the coverage area. To this end, it is assumed that each of the K simultaneously served users is located in a different beam footprint. Only atmospheric fading due to rain is considered in the user link. In particular we consider the fading statistic of the city of Rome, as provided in [7]. Eventually, the numerical results will provide system performance measures averaged out on the fading and UTs locations statistics (by considering ten thousand fading/locations realizations).

We focus on two conventional performance metrics: (i) throughput (bit/s) and (ii) availability. In accordance with the current practice, we will deduce both these metrics from Table I which provides a one-to-one relationship between the required received SINR and the efficiency[4] (bits/symbol) achieved by the different adaptive modulation and coding modes included in the DVB-S2 standard, for a packet error rate (PER) of 10^{-6}. Note that the working points were extrapolated from the PER curves reported in the DVB-S2 guidelines document [8] with some additional approximate implementations losses [1]. The rest of parameters used in the simulation are summarized in Table II. Among them, note that the total bandwidth $B_T = 500$MHz is assumed to be divided into $M = 12$ carriers. Still, the throughput results will be presented for the total bandwidth (i.e. by summing the contribution of each carrier) and as a function of the total power denoted by P_T which accounts for the transmit power of all carriers $P_T = MP$.

In the sequel, the different precoders and scenarios described in the previous sections will be compared to each other, but also contrasted to a reference scenario designed according to the current best practice. The features of the chosen reference scenario are (i) fixed on-board beamforming $\mathbf{B}$, (ii) no precoding, (iii) frequency reuse pattern with $N_c = 3$.

B. Perfect Channel State Information

Let us assume first that the channel is perfectly known at the GW. Fig. 1 first compares the regularized channel inversion and ZF linear precoder. The regularized channel inversion significantly outperforms the more naive ZF precoder. Most importantly, the benefit of the joint precoding and beamforming design is apparent both in terms of throughput and availability. For instance, at $P_T = 30$dBW the regularized channel inversion in the feed space generates a 111% relative throughput increase with respect to the reference scenario, and 17% with respect to the same processing in the beam space. However, a slight decrease in system availability can still be observed with respect to the reference scenario.

Fig. 2 considers the MMSE precoders described in Subsection III-C, and illustrates again the benefit of the proposed joint

[4]Excluding efficiency loss due to preamble and pilot insertion.

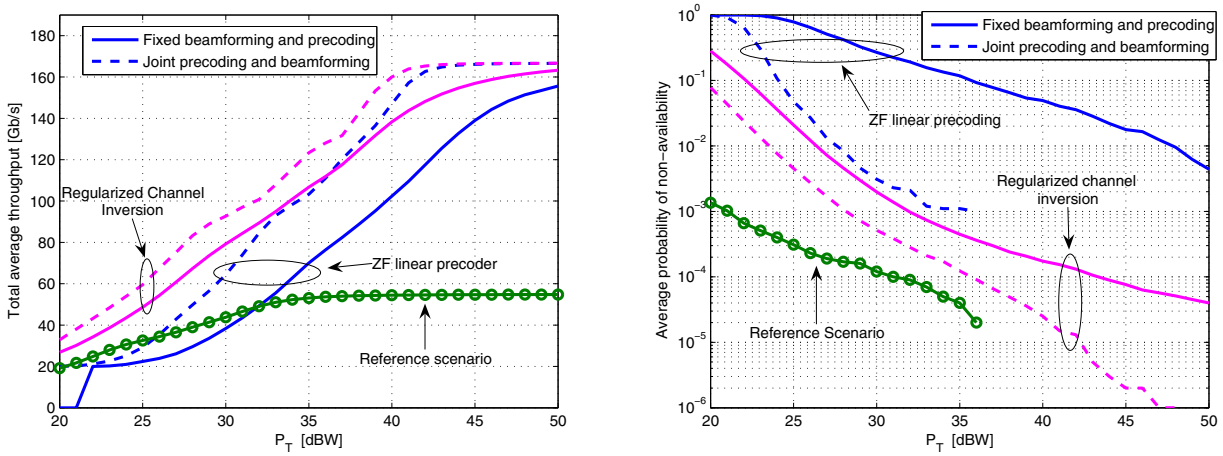

Fig. 1. Regularized channel inversion and ZF linear precoding in beam and feed space: throughput and availability comparison with perfect CSI.

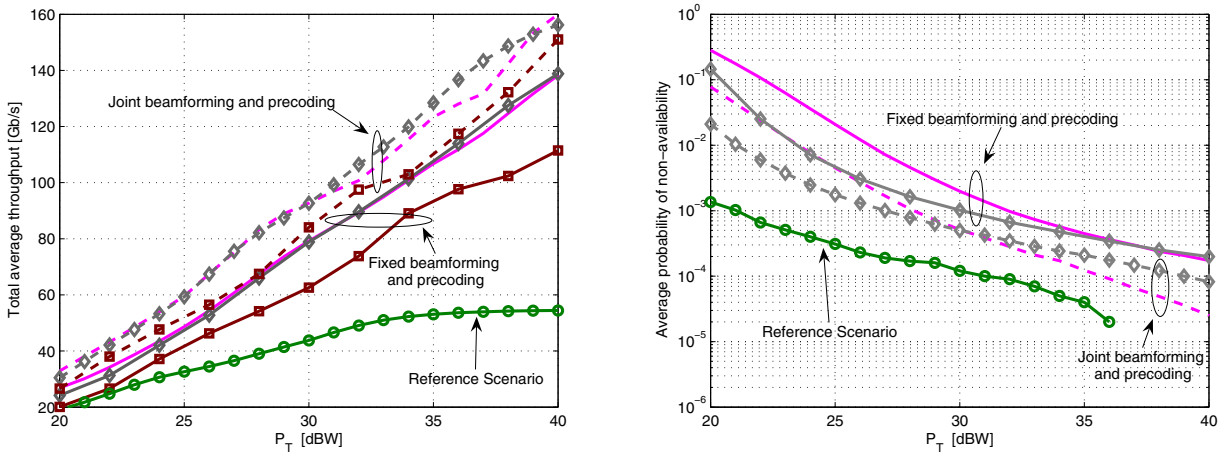

Fig. 2. Throughput and availability comparison with perfect CSI. Legend: no marker - regularized channel inversion, ♢ - UpConst MMSE precoder, □ - Equal SINR MMSE precoder.

design. On the one hand, it can be seen that the comparison between the regularized channel inversion and UpConst MMSE precoders depends on the value of P_T: in terms of availability, the regularized channel inversion outperforms the UpConst MMSE precoder at high SNR, and viceversa at low SNR. On the other hand, the Equal SINR MMSE precoder achieves a full system availability (and therefore is not depicted in the right part of Fig. 2) at the expense of a non-negligible loss in throughput (with respect to other precoders). The reason is that, with such precoder, a single UT with unfavorable channel/interfence conditions can bring down the throughput for all UTs.

C. Imperfect Channel State Information

In this subsection, we disregard the assumption of perfect CSI at the GW, and analyze the robustness of the different schemes to channel estimation errors. We consider that the precoder design is now based on a feed channel estimate $\hat{\mathbf{H}}_f = \mathbf{H}_f + \mathbf{E}_f$ (or $\hat{\mathbf{H}}_b = \mathbf{H}_b + \mathbf{E}_b$ in the beam space). Each row of $\hat{\mathbf{H}}_f$ (or $\hat{\mathbf{H}}_b$) is based on a channel estimation which is carried out separately at each UT and then reported to the GW via the return link (assumed ideal). Note that the reporting of $\hat{\mathbf{H}}_f$ to the GW implies feeding back $(N-K)K$ more channel samples than for reporting $\hat{\mathbf{H}}_b$. We assume L-length orthogonal training sequences, such that the entries of $\mathbf{E}_f$ (or $\mathbf{E}_b$) are i.i.d zero mean complex circular symmetric Gaussian random variables with variance inversely proportional to L [9].

Fig. 3 depicts the achievable throughput and system availability for $L = 256$. The joint design still appears beneficial, especially throughput wise. However, only the Equal SINR MMSE precoder is able to achieve an availability level close to the reference scenario. The regularized channel inversion appears to be more robust to imperfect CSI than the precoders based on the uplink-downlink duality. Table III provides all results (including for $L = 1024$) for $P_T = 30$dBW. With the regularized channel inversion, the relative throughput increase generated by the feed processing with respect to the beam processing is of the order of 17% for perfect CSI, 20% for $L = 1024$, and 24% for $L = 256$. Quite surprisingly, the relative throughput gain generated by the joint design increases as the degree of CSI decreases, illustrating the feed processing with regularized channel inversion.

TABLE III
NUMERICAL COMPARISON FOR TOTAL TRANSMIT POWER $P_T = 30dBW$

Scenario		Perfect CSI		Imperfect CSI, $L = 1024$		Imperfect CSI, $L = 256$	
Beamforming	**Precoding**	**Total Average Troughput** [Gb/s]	**Average Availability** [%]	**Total Average Troughput** [Gb/s]	**Average Availability** [%]	**Total Average Troughput** [Gb/s]	**Average Availability** [%]
Fixed	Regularized channel inversion	79.22	99.79	75.23	99.75	63.11	99.53
	UpConst MMSE	78.85	99.90	74.44	99.85	62.09	99.73
	Equal SINR MMSE	62.59	100	60.52	99.99	54.39	99.96
Joint beamforming & precoding	Regularized channel inversion	92.69	99.94	90.19	99.94	77.99	99.88
	UpConst MMSE	92.67	99.95	88.84	99.91	79.63	99.76
	Equal SINR MMSE	84.05	100	80.10	99.99	68.56	99.97
Reference scenario		43.78	99.99	43.78	99.99	43.78	99.99

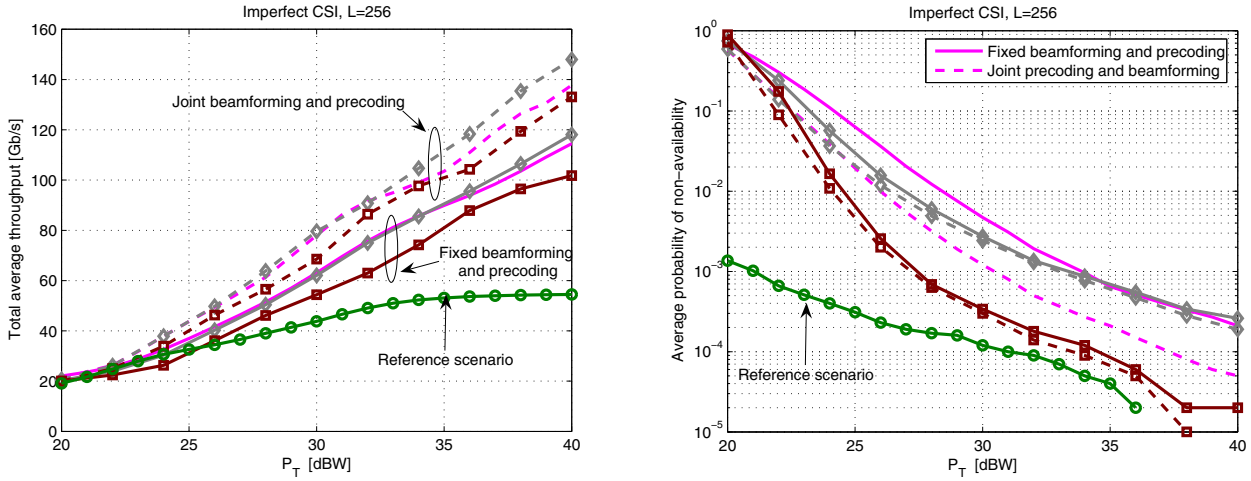

Fig. 3. Throughput and availability comparison with imperfect CSI ($L = 256$). Legend: no marker - regularized channel inversion, ♢ - UpConst MMSE precoder, □ - Equal SINR MMSE precoder.

V. CONCLUSIONS

This paper proposed the joint design of linear precoding and ground based beamforming (or equivalently linear precoding in the feed space) to mitigate the interference among users in next generation multi-beam broadband satellite systems. It was shown how this joint design improves the performance both in terms of throughput and availability. Out of all the linear precoders that have been considered, the regularized channel inversion seemed to reach the best trade-off between performance and complexity. Most importantly, it appeared to be more robust to imperfect CSI than MMSE precoders which are based on the uplink-downlink duality.

Note that the focus of this paper was on the forward link, but the return link has also been considered in a parallel activity. Finally, let us stress that the proposed joint design assumes that all feed signals are available on-ground, which implies a higher feeder link bandwidth than conventional schemes. The introduction of a feeder link bandwidth constraint is an open issue which is currently being studied.

ACKNOWLEDGMENT

The authors would like to thank Riccardo De Gaudenzi from the European Space Agency for his comments and suggestions.

REFERENCES

[1] G. Gallinaro *et al.*, "Novel intra-system interference mitigation techniques and technologies for next generations broadband satellite systems," Final report of ESA/ESTEC contract No. 18070/04/NL/US, 2008.

[2] L. Cottatellucci *et al.*, "Interference mitigation techniques for broadband satellite systems," in *Proc. 24th AIAA Int. Commun. Satell. Systems Conf., ICSSC*, Jun. 2006.

[3] P. Angeletti and N. Alagha, "Space/ground beamforming techniques for emerging hybrid satellite terrestrial networks," in *Proc. 27th AIAA Int. Commun. Satell. Systems Conf., ICSSC*, Edinburgh, UK, Jun. 2009.

[4] C. Peel, B. Hochwald, and A. Swindlehurst, "A vector-perturbation technique for near-capacity multiantenna multiuser communication - part I: channel inversion and regularization," *IEEE Trans. Commun.*, vol. 53, no. 1, pp. 195 – 202, jan. 2005.

[5] P.Viswanath and D.N.C.Tse, "Sum capacity of the vector Gaussian broadcast channel and uplink-downlink duality," *IEEE Trans. Inf. Theory*, vol. 49, no. 8, pp. 1912–1921, Aug. 2003.

[6] G. Caire and L. Cottatellucci and M. Debbah and G. Lechner and R. Muller, "Interference mitigation techniques for satellite systems," Technical report of ESA/ESTEC contract No. 18070/04/NL/US, 2005.

[7] N. Zorba, M. Realp, and A. Pérez-Neira, "An improved partial CSIT random beamforming for multibeam satellite systems," in *Proc. 10th Int. Work. Signal. Process. Space Commun., SPSC*, Oct. 2008.

[8] "DVB-S2: Digital video broadcasting (DVB) user guidelines for the second generation system for broadcasting, interactive services, news gathering and other broadband satellite applications (DVB-S2)," ETSI TR 102 376.

[9] M. Bergmann, W. Gappmair, C. Mosquera, and O. Koudelka, "Channel estimation on the forward link of multi-beam satellite systems," in *Proc. 3rd International ICST Conference on Personal Satellite Services (PSATS)*, Malaga, Spain, Feb. 2011.